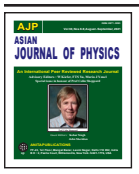

Asian Journal of Physics
Vol. 30, Nos 8 & 9 (2021) 1355-1364
Available on: www.asianjournalofphysics.com

ap

Realizing singular beams through dual-pass phase modulation

Praveen Kumar and Naveen K Nishchal

Department of Physics, Indian Institute of Technology Patna, Bihta, Patna-801 106*, Bihar, India*

Dedicated to Prof CJR Sheppard

Singular optics has become a widely researched area because of many applications of optical vortices and the orbital angular momentum. In optics, singularity emerges in connection with optical fields with spatial inhomogeneity. For this reason, the concept of light beam shaping occupies a prominent position in singular optics. One of the important aspects of current research is the efficient technique to realize vector fields of light having structured polarization. This paper describes the dual-pass phase modulation technique for generating vector fields having phase and polarization singularities. Simulation and experimental results of singular beams have been presented.

Keywords: Optical vortices, Vector-vortex beams, Optical singularity, Spatial light modulator, Polarization.

1 Introduction

Advancement in technology to produce well-defined light beams has attracted significant attention. For this reason, laser beams have occupied prominent positions in many optical technologies. Different parameters describing optical fields can be tailored spatially and temporally. Intensity, phase, and polarization are the parameters of light that can be shaped uniquely for a purpose. Such light beams are referred to as structured light or tailored light [1]. Many efforts are being made for the wavefront shaping of laser beams [1-3].

Recent efforts have uncovered many new features of optical fields which are associated with their unique spatial distribution such as optical singularity [4,5]. The foundation for the study of optical singularity or wavefront dislocations was laid by the pioneering work of Nye and Berry in 1974 [6]. Later, Coullet *et al* introduced the term 'optical vortex' for phase singularity. At the singular points, the phase remain indeterminate [7]. A point in optical field at which both phase and polarization singularity simultaneously exist is referred to vector-vortex [8]. Vector fields of light have spatially inhomogeneous polarization distributions. Light beams embedded with singularity are referred to as the singular beams. Many active investigations on fundamental theories and applications of singular beams are currently undergoing in various platforms [9-11].

Singular beams have brought up many innovations among them the most attractive is their association with the orbital angular momentum (OAM) of light [12]. In 1992, Allen *et al* realized in their study that the light with helical wavefront carries well-defined OAM per photon [13]. The combination of the concept of OAM with the idea of optical vortices have created new possibilities in classical and quantum optics [12,14-17]. Singular beams have found applications in optical manipulation [18], optical communications [19], metrology [20], and microscopy [21]. They play a crucial role in the study of light-matter interactions, spin-orbit interactions [22], and quantum optics [23]. Significant developments with the fundamental theories

Corresponding author
e mail: nkn@iitp.ac.in (Naveen K Nishchal)

and applications of singular beams have been reported in recent articles [24-28]. An efficient and convenient technique for beam shaping is a prerequisite for emerging innovations and applications of singular beams. In recent years, spatial light modulators (SLM) have become popular for beam shaping because of their capability to control the wavefront of light flexibly [29,30]. The wavefront of incident laser beams can be converted to helical that holds an optical vortex. Further, different techniques can be applied to utilize the SLM to manipulate the polarization distribution of light [31,32]. A common way to realize vector fields is through the superposition of scalar fields on an orthogonal polarization basis. Off late, non-interferometric approaches such as the technique of dual-pass phase modulation have emerged to simplify the optical set-ups for the efficient generation of vector fields with singularity [33,34].

This paper describes the generation of singular beams using SLM. The technique of dual-pass phase modulation has been explained, which can be used to realize vector-vortex beams. This technique uses a compact and non-interferometric experimental set-up with a single SLM. The presented methods are useful for generating different orders of singular beams. The rest of the paper is organized as follows: Sections 2 and 3 describe the optical singularity and singular beams, respectively. The generation of singular beams using SLM has been presented in section 4. Finally, some conclusions are drawn in Section 5.

2 Optical singularity

In optics, a singularity refers to a point in the electromagnetic field at which some parameters that describes the field becomes indeterminate; however, a circulating gradient of parameter surrounds the singular point. Commonly known singularity points in optics are associated with the phase and the polarization [4,25,26].

2.1. Phase singularity

In the optical field, the point of phase singularity occurs where the phase is indeterminate and the gradient of phase circulates around the singularity [35,36]. At the phase singularity, the amplitude of light remains zero, which appears as isolated dark intensity spots. The optical vortex is formed at the singularity because of the helical wavefront of light. The optical fields can have different orders of phase singularity depending on the wavefront helicity. Phase singularity can also be found in the optical fields formed by interference of multiple beams [37].

2.2. Polarization singularity

The state of polarization (SOP) of light can be characterized by two parameters: the orientation angle of the major axis and the ellipticity angle of the polarization ellipse. Polarization singularities arise because of the ambiguity in parameters used to characterize the SOP in a vector field of light [38,39]. Depending on the polarization distribution of the optical field around the singularity points, they can be classified as C-points or V-points. At a C-point, the SOP is circular, and therefore the azimuth of the polarization ellipse is indeterminate. Polarization distribution around a C-point consists of SOPs with spatially varying orientation angle and non-zero ellipticity angle. The orientation angle becomes indeterminate at a V-point. It arises in a vector fields where the SOPs are predominantly linear. V-point occurs at an intensity null-point around which the orientation angle of SOPs undergoes rotation [40-42]. Optical fields may also possess L-line singularity where the handedness of polarization ellipse remains undefined.

3 Singular beams

For decades, singular beams which hold optical singularities have been a topic of considerable interest. Such beams can be homogeneously polarized or inhomogeneously polarized and can be referred to as (scalar) vortex beams and vector-vortex beams, respectively) [29]. They are described in the following sub-sections:

3.1 Vortex beams

Optical vortex beams are produced when the light with helical wavefront rotates like a corkscrew around the phase singularity that lies along the propagation axis [13]. Vortex beams have many unique properties among which their association with singularity and the OAM are most widely explored.

Laguerre-Gaussian (LG) modes have a helical phase profile, hence holds an optical vortex [14]. They are the paraxial solutions of the scalar Helmholtz equation. The electric field amplitude of LG mode which propagates along the z-direction, can be expressed as,

$$E^{LG}(x, y, l) = \sqrt{\frac{2p!}{\pi(p+|l|)!}} \frac{1}{w(z)} \left[\frac{r\sqrt{2}}{w(z)}\right]^{|l|} \exp\left[\frac{-r^2}{w^2(z)}\right] L_p^{|l|}\left(\frac{2r^2}{w^2(z)}\right) \exp\left[\frac{ik_0 r^2 z}{2(z^2+z_R^2)} - i\psi + il\phi\right] \quad (1)$$

In this equation, $r = \sqrt{x^2+y^2}$ and ϕ denotes the azimuth angle, given as $\phi = \tan^{-1}(y/x)$. l is the azimuthal index, also referred to as the topological charge (TC). The term $w(z)$ is the $1/e$ radius of Gaussian term, which is given by $w(z) = w(0)\,[(z^2 + Z_R^2)/Z_R^2]^{1/2}$, where $w(0)$ denotes beam waist and Z_R is the Rayleigh range. ψ is Gouy phase given by $\psi = (2p + |l| + 1)\tan^{-1}(z/z_R)$. The term $L_p^{|l|}$ is the associated Laguerre polynomial where p denotes the radial index.

TC is an important parameter of vortex beams that specifies the order of phase singularity and the amount of OAM carried by the beam [36,43,44]. Figure 1 shows the phase and intensity profiles of different orders of vortex beam. They have a doughnut-shaped intensity profile resulting from the phase singularity.

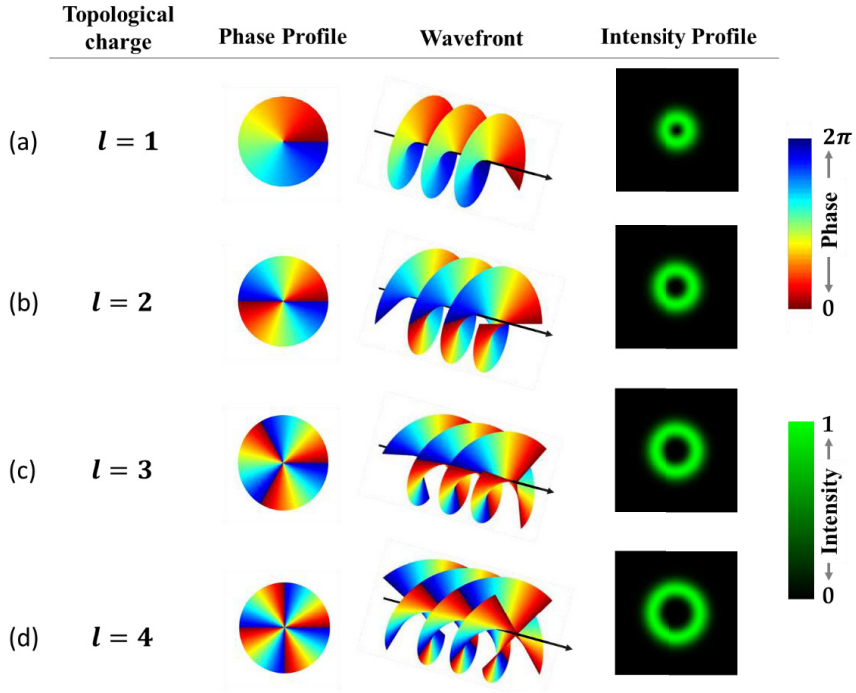

Fig 1. Vortex beams of different orders of topological charge

As illustrated in Fig 1, the singularity in phase arises at a point around which the phase changes by the signed integral multiple of 2π. The magnitude of TC is equal to the number of windings of the phase per revolution around the singular point. The direction in which the phase increases gives the sign of TC. For an opposite sign of TC, the phase increases in the opposite direction around the singular point.

3.2. Vector-vortex beams

Vector-vortex beams have spatially inhomogeneous polarization distribution and have both phase and polarization singularity [8]. Their unique properties are of great interest for various applications such as focusing, microscopy, optical manipulation, material processing, and imaging [45]. A special class of vector-vortex beams are cylindrical-vector (CV) beams [46]. They are the paraxial solutions of the vector Helmholtz equation and have axial symmetry in both amplitude and phase. Commonly known CV beams have radial and azimuthal polarization distributions. In addition to phase singularity, they hold V-points. CV beams, when projected onto a Poincaré sphere, span the equator. Another type of vector-vortex beams that hold C-points and spans the entire surface of the Poincaré sphere are the Full Poincaré beams [47]. Mathematically, the vector-vortex beams embedded with V-points and C-points can be described by the superposition of LG modes in the circular polarization basis. Their optical fields can be represented using the Jones matrix as follows:

$$\begin{bmatrix} E_1^{LG} \\ E_2^{LG} \end{bmatrix} = \begin{bmatrix} 1-i & -1-i \\ -1-i & 1-i \end{bmatrix} \begin{bmatrix} E^{LG}(x, y; l_1) \\ E^{LG}(x, y; l_2)\exp(i\delta) \end{bmatrix} \tag{2}$$

where $E^{LG}(x, y, l_1)$ and $E^{LG}(x, y, l_2)$ denote the complex field amplitudes of LG modes given by Eq (1). Appropriate selection of TCs l_1, l_2 and additional phase delay δ in Eq (2) describes beams with different orders of polarization singularity. A V-point is created when l_1 and l_2 have equal magnitudes but opposite sign. While in the case of a C-point, either of TCs l_1 or l_2 remains zero. The simulated intensity and polarization profiles of the commonly known vector-vortex beams are shown in Figs 2 and 3. CV beams are presented in Fig 2. In this figure, the CV beams presented in rows (a) to (d) are referred to as Type I, II, III, and IV, respectively [27,33]. Each of them has different polarization distributions around the V-points. Type I and Type III represent well-known azimuthally and radially polarized beams, respectively. They have Poincaré-Hopf or V-point singularity index +1, whereas it is –1 for Type II and Type IV. Figure 3 shows the Poincaré beams. Rows (a-b) represent the polarization distributions referred to as star, while the rows (c-d) represent lemon. C-point singularity index of lemon is 1/2, whereas it is –1/2 for the star [27,48].

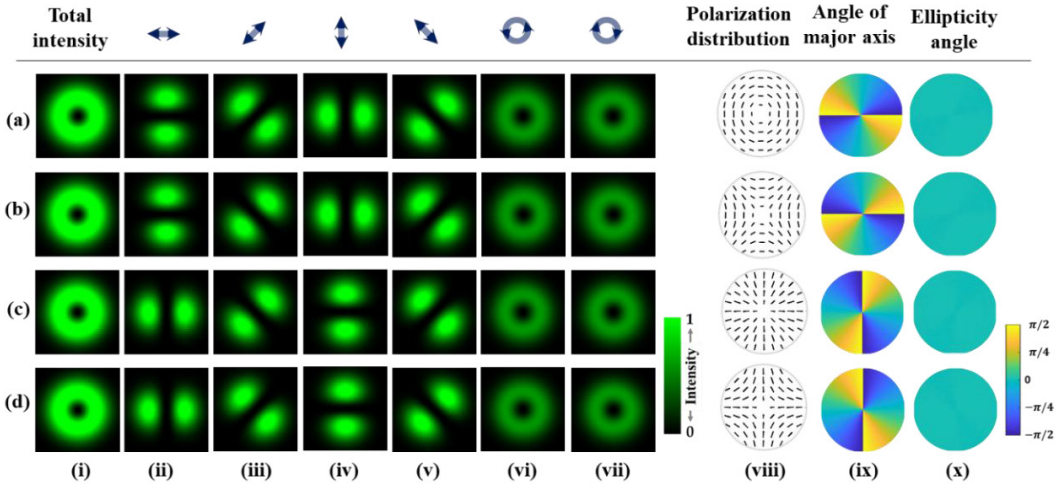

Fig 2. Simulated intensity and polarization distributions of CV beams having V-points. Rows (a) to (d) correspond to Type I, II, III, and IV, respectively. Column (i) shows the total intensity of beam. Columns (ii)-(vii) show the intensity when the beam is analyzed using a QWP and a polarizing filter at different sets of retardation and polarizer alignment angle. Column (viii) shows polarization distributions. Columns (ix) and (x) present polarization azimuth angle and ellipticity angle distributions, respectively.

Polarization singularity index is the measure of periodic variations in the SOP around the singular point. The index sign depends on the direction in which the major axis of the polarization ellipse changes gradually around the singular point. Its magnitude depends on the amount of rotation of the major axis around the singularity. For CV beams, the ellipticity angle of the polarization ellipse at different spatial locations remains uniformly zero while it is non-uniform for the case of Poincaré beams. It has been illustrated in the polarization distributions shown in Figs 2 and 3.

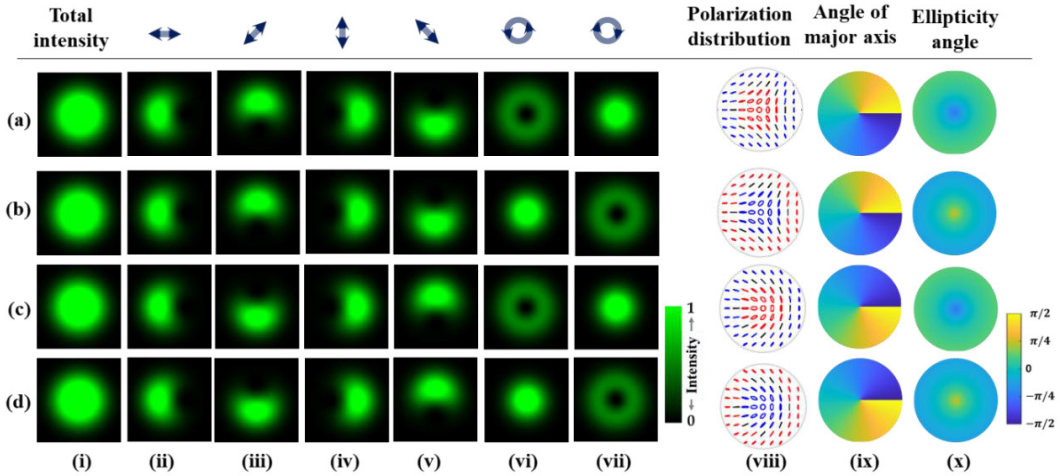

Fig 3. Simulated intensity and polarization distributions of Poincaré beams having C-points. Rows (a-b) represent star, and (c-d) represent lemon. Column (i) shows the total intensity of beam. Columns (ii)-(vii) show the intensity when the beam is analyzed using a QWP and a polarizing filter at different sets of retardation and polarizer alignment angle. Column (viii) shows polarization distributions. Columns (ix) and (x) represent polarization azimuth angle and ellipticity angle distributions, respectively. Red and blue colors in polarization distribution represent the opposite sign of ellipticity angle.

4 Generation of singular beams

There has been an effort to generate singular beams in an efficient and controlled way owing to various applications. Recent advances in techniques of beam shaping have made singular beams a practical reality. Laser beams with dislocations can be generated using diffractive holograms consisting of fork-shaped gratings or spiral Fresnel zone plates [11]. Spiral phase plates or vortex phase masks have also been used to convert the laser beam into a helical wavefront [49]. CV beams can be realized using Q-plates [48]. Recently, electro-optic devices such as SLM have gained importance for their ability to flexibly generate different orders of singular beams [50,51]. The SLM and the technique of dual-pass phase modulation for realizing vector-vortex beams have been described in the subsequent sections.

4.1 Spatial light modulator

SLMs are pixelated displays that can be used for phase-only modulation of incident light beam [50,52]. They act as a phase retarder that induces phase delay to an incoming light wave. Birefringent characteristics of liquid crystal (LC) based SLM allow phase modulation of specific polarization component, which can be utilised for polarization shaping [51]. LC molecules are rod-shaped and have variations in the refractive index, which is maximal along their long axis, also referred to as the slow axis . In this study, a reflective-type LC SLM (Pluto Holoeye, Germany) has been used to generate singular beams. This SLM has a resolution of 1920×1080 pixels and a pixel pitch of 8.0 μm. Mathematically, the Jones matrix of a phase-only SLM can be represented as follows [50].

$$J = \begin{bmatrix} \exp\{i\phi(x, y)\} & 0 \\ 0 & 1 \end{bmatrix} \tag{3}$$

where $\phi(x, y)$ is the phase delay introduced by the SLM. Control of phase delay at each pixel of the SLM's display allows spatially dependent phase modulation. The induced phase delay is controlled through the computer-generated hologram (CGH), which can be displayed on the screen of a computer to which the SLM is connected as the second screen. The CGH consists of an 8-bit image having 256 gray levels from 0 (black) to 255 (white), which is usually associated with the discrete increments of the phase shift value from 0 to 2π through a linear relationship [53,54]. Desired two-dimensional phase profile distributions can be modulated into the light by simply displaying the CGH onto the SLM.

4.2 Dual-pass phase modulation technique

SLM can be used for the polarization shaping of light beam through on-axis configuration [32,33]. For realizing CV beams, modulation of both the orthogonal polarization components is required. The LC SLM used in this study modulates only one of the components at a time and, therefore, the technique of dual-pass phase modulation is incorporated to achieve the modulation of both orthogonal polarization components [33]. CV beams and Poincaré beams can be realized through the superposition of two LG modes on a circular polarization basis. The optical field components E_1^o and E_2^o of the resultant beam can be represented in terms of Jones formalism as,

$$\begin{bmatrix} E_1^o(x, y) \\ E_2^o(x, y) \end{bmatrix} = \frac{1}{2} \begin{bmatrix} 1 - i & -1 - i \\ -1 - i & 1 - i \end{bmatrix} \begin{bmatrix} A_x \exp\{i\phi_x(x, y)\} \\ A_y \exp\{i\phi_y(x, y)\} \end{bmatrix} \tag{4}$$

where $\phi_x(x, y)$, $\phi_y(x, y)$ denote the phase distributions and A_x, A_y denote amplitudes. The optical fields E_1^o and E_2^o, when propagates a short distance; then the resulting field at that distance can be estimated by Fresnel diffraction solution.

The schematic of the experimental set-up for realizing vector-vortex beams using the technique of dual-pass phase modulation is shown in Fig 4(a). The picture of the actual set-up is shown in Fig 4(b). In this case, CGH to be modulated into the SLM is prepared using the grayscale image of phase distributions, ϕ_x and ϕ_y, which are placed side-by-side. A collimated laser beam diameter of ~ 4 mm is directed towards the SLM's display through a non-polarizing beam splitter (Thorlabs BS013 of size 25.4 mm). The beam is linearly polarized at 45° with the slow axis of SLM. In the first reflection, the SLM modulates only one of the components and simply reflects the other. After transmitting through a half-wave plate (HWP), the beam is redirected using a right-angle prism (Thorlabs PS911 of size 25 mm) towards the other half of the SLM's display to modulate the other component. Thus, after the second reflection, the PVDs $\phi_x(x, y)$ and $\phi_y(x, y)$ are modulated into the x- and y-components of the light beam, respectively. The beam then transmits through a quarter-wave plate for polarization basis conversion. Additional phase-shift and flip is introduced in the wavefront of light after it transmits through prism. The CGH is designed accordingly for its correction. A radially polarized vector field is generated by modulating the phase distributions as follows:

$$\begin{aligned} \phi_x &= \tan^{-1}(y/x) \\ \phi_y &= \tan^{-1}(y/x) + \pi/2 \end{aligned} \tag{5}$$

The CGH displayed onto the SLM for this case is shown in Fig 4(c). The intensity distributions of the resulting beam are captured at different orientations of the polarizer to analyze the polarization distribution. The captured intensity distributions have a petal-shaped pattern because of the spatially varying polarization as shown in Figs 5(a)-(d). The intensity distribution captured without the polarizer is shown in Fig 5(e). The polarization distribution of a radially polarized beam is presented in Fig 5(f). It shows the dark intensity region at the center, which results due to the presence of vortices that indicate the presence of phase singularity. At this point, the optical field has both phase and polarization singularities.

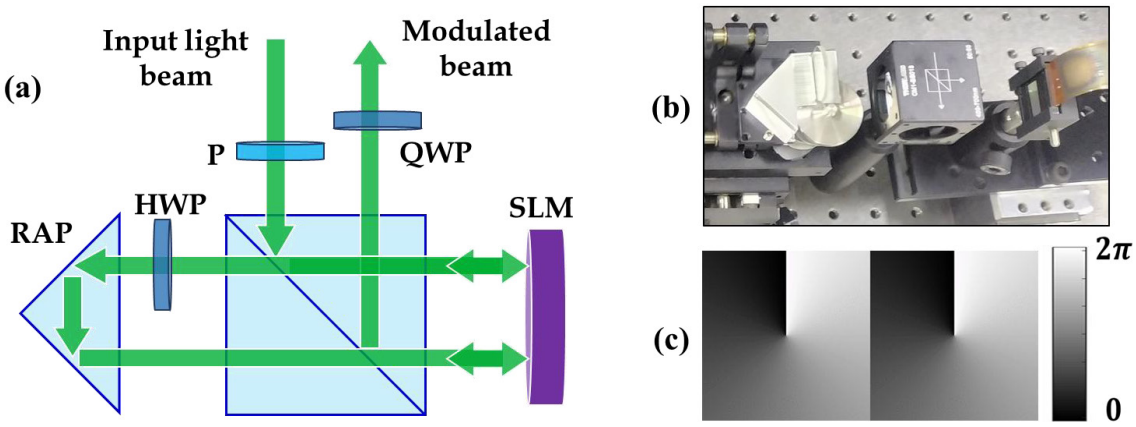

Fig 4. (a) Schematic of the experimental set-up, P: Polarizer, HWP: Half wave plate, RAP: Right angle prism, and QWP: Quarter wave plate, (b) picture of actual set-up, and (c) CGH displayed onto the SLM.

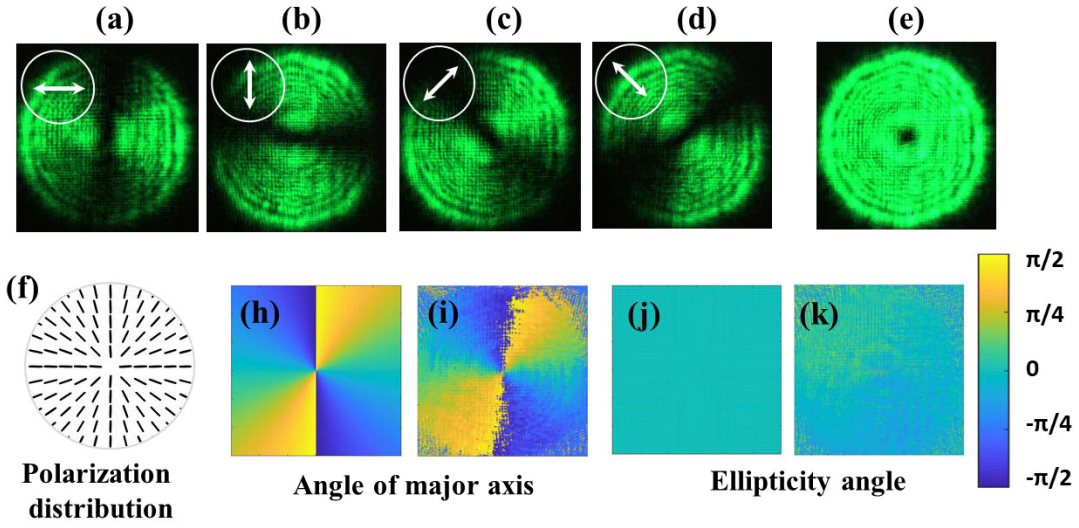

Fig 5. Results of experimentally generated radially polarized CV beam. (a-d) show the recorded intensity distribution at different orientations of a linear polarizer and (e) intensity without using a polarizer. (f) shows simulated polarization distribution. (h-k) shows distributions of polarization angle parameters. (h) and (j) present simulation results. (i) and (k) present experimental results.

To further analyze the quality of the beam, the distribution of angular parameters of polarization ellipse has been obtained through Stokes polarimetry [33]. Since the generated beam is radially polarized, the major axis orientation of the polarization ellipse has azimuthal angle dependence and lies within [–π/2 π/2] as shown in Fig 5(h). Since the SOP of a vector beam is predominantly linear, the ellipticity angle remains uniformly zero as shown in Fig 5(j). These parameters are experimentally measured and are presented in Figs 5(i) and (k). It can be observed that the simulated and experimentally obtained distributions are in good agreement with each other and hence verify the generated radially polarized vector field. The technique of dual-pass phase modulation can also be used to produce arbitrary vector beams, which have recently gained significant interest in information encoding and security applications [51,55,56].

5 Conclusion and remarks

SLM offers convenience and flexibility for generating singular beams. The technique of dual-pass phase modulation requires a single LC SLM for realizing vector-vortex beams. Since it is a non-interferometric approach, it allows stable phase modulation and are less sensitive to external vibrations. This feature helps generate high-order singular beams. Besides, the alignment is more convenient than the techniques based on the superposition of scalar modes. The technique of dual-pass phase modulation can be also used to generate non-singular vector beams. Therefore, it could be a subject of interest in other areas of optics.

References

1. Rubinsztein-Dunlop H, Forbes A, Berry M V, Dennis M R, Andrews D L, Mansuripur M, Denz C, Alpmann C, Banzer P, Bauer T, Karimi E, Marrucci L, Padgett M, Ritsch-Marte M, Litchinitser N M, Bigelow N P, Rosales-Guzmán C, Belmonte A, Torres J P, Neely T W, Baker m, Gordon R, Stilgoe A B, Romero J, White A G, Fickler R, Willner A E, Xie G, McMorran B, Weiner A M, Roadmap on structured light, *J Opt*, 19(2017)013001; doi.org/10.1088/2040-8978/19/1/013001.
2. Andrews D L, Structured Light and Its Applications, (Elsevier) 2008.
3. Angelsky O V, Bekshaev A Y, Hanson S G, Zenkova C Y, Mokhun II, Jun Z, Structured light: Ideas and concepts, *Front Phys*, 8(2020)114; doi.org/10.3389/fphy.2020.00114.
4. Dennis M R, O'Holleran K, Padgett M J, Singular optics: Optical vortices and polarization singularities, Progr *Opt*, 53(2009)293–363.
5. Soskin M S, Vasnetsov M V, Singular optics, *Progr Opt*, 42(2001)219–276.
6. Nye J F, Berry M V, Dislocations in wave trains, *Proc R Soc London A*, 336(1974)165–190.
7. Coullet P, Gil L, Rocca F, Optical vortices, *Opt Commun*, 73(1989)403–408.
8. Prati F, Tissoni G, San Miguel M, Abraham N B, Vector vortices and polarization state of low-order transverse modes in a VCSEL, *Opt Commun*, 143(1997)133–146.
9. Vasnetsov M V, Staliunas K, Optical Vortices, (Nova Science Publ.), 1999.
10. Kotlyar V V, Kovalev A A, Porfirev A P, Vortex Laser Beams, (CRC Press) 2018; doi.org/10.1201/9781351009607.
11. Shen Y, Wang X, Xie Z, Min C, Fu X, Liu Q, Gong M, Yuan X, Optical vortices 30 years on: OAM manipulation from topological charge to multiple singularities, *Light Sci Appl*, 8(2019)90; doi.org/10.1038/s41377-019-0194-2.
12. Allen L, Barnett S M, Padgett M J (Eds), Optical Angular Momentum, (IOP Publ. UK), 2003.
13. Allen L, Beijersbergen M W, Spreeuw R J C, Woerdman J P, Orbital angular momentum of light and the transformation of Laguerre-Gaussian laser modes, *Phys Rev A*, 45(1992)8185–8189.
14. Yao A M, Padgett M J, Orbital angular momentum: origins, behavior and applications, *Adv Opt Photon*, 3(2011)161–204.
15. Torner L, Torres J P, Twisted Photons, (Wiley Publ.), 2011.
16. Andrew D L, Babiker M, The Angular Momentum of Light, (Cambridge University Press), 2013.
17. Padgett M J, Orbital angular momentum 25 years on, *Opt Express*, 25(2017)11265–11274.
18. Dholakia K, Čižmár T, Shaping the future of manipulation, *Nat Photon*, 5(2011)335–342.
19. Wang J, Advances in communications using optical vortices, *Photon Res*, 4(2016)B14–B28.
20. Rosales-Guzmán C, Hermosa N, Belmonte A, Torres J P, Experimental detection of transverse particle movement with structured light, *Sci Rep*, 3(2013)2815; doi/org/10.1038/srep02815.
21. Fürhapter S, Jesacher A, Bernet S, Ritsch-Marte M, Spiral phase contrast imaging in microscopy, *Opt Express*, 13(2005)689–694.
22. Marrucci L, Manzo C, Paparo D, Optical spin-to-orbital angular momentum conversion in inhomogeneous anisotropic media, *Phys Rev Lett*, 96(2006)163905; doi.org/10.1103/PhysRevLett.96.163905
23. Molina-Terriza G, Torres J P, Torner L, Twisted photons, *Nat Phys*, 3(2007)305–310.
24. Gbur G, Singular Optics-The Optics Encyclopedia, (Wiley Publ.), 2015.
25. Soskin M S, Boriskina S V, Chong Y, Dennis M R, Desyatnikov A, Singular optics and topological photonics, *J Opt*, 19(2017)010401; doi.org/10.1088/2040-8986/19/1/010401.

26. Gbur G J, Singular Optics, (CRC Press), 2017.
27. Senthilkumaran P, Singularities in Physics and Engineering, (IOP Publ. UK), 2018.
28. Kumar P, Nishchal N K, Singh K, Role of self-referenced interferometry in measuring the orbital angular momentum of optical vortices: A review, *Asian J Phys*, 29(2020)835-852.
29. Pachava S, Dharmavarapu R, Vijayakumar A, Jayakumar S, Manthalkar A, Dixit A, Viswanathan N K, Srinivasan B, Shanti Bhattacharya S, Generation and decomposition of scalar and vector modes carrying orbital angular momentum: a review, *Opt Eng*, 59(2019)041205; doi.org/10.1117/1.OE.59.4.041205.
30. Kumar P, Nishchal N K, Array formation of optical vortices using in-line phase modulation, *Opt Commun*, 493(2021)127020; doi.org/10.1016/j.optcom.2021.127020.
31. García-Martínez P, Marco D, Martínez-Fuentes J L, Sánchez-López M M, Moreno I, Efficient on-axis SLM engineering of optical vector modes, *Opt Lasers Eng*, 125(2020)105859; doi.org/10.1016/j.optlaseng.2019.105859.
32. Kumar P, Pal S K, Nishchal N K, Senthilkumaran P, Formation of polarization singularity lattice through dual-phase modulation, *J Opt*, 22(2020)115701; doi.org/10.1088/2040-8986/abbb5d.
33. Kumar P, Pal S K, Nishchal N K, Senthilkumaran P, Non-interferometric technique to realize vector beams embedded with polarization singularities, *J Opt Soc Am A*, 37(2020)1043–1052.
34. Wu D, Li Y, Jia W, Zhou J, Zhao Y, Fu Y, Wang J, Generation of arbitrary vector vortex beams based on the dual-modulation method, *Appl Opt*, 58(2019)1508–1513.
35. Bazhenov V Y, Vasnetsov M V, Soskin M S, Laser beams with screw dislocations in their wavefronts, *JETP Lett*, 52(1990)152–154.
36. Soskin M S, Gorshkov V N, Vasnetsov M V, Malos J T, Heckenberg N R, Topological charge and angular momentum of light beams carrying optical vortices, *Phys Rev A*, 59(1997)4064–4075.
37. O'Holleran K, Padgett M J, Dennis M R, Topology of optical vortex lines formed by the interference of three, four, and five plane waves, *Opt Express*, 14(2006)3039–3044.
38. Mokhun A I, Soskin M S, Freund I, Elliptic critical points: C-points, a-lines, and the sign rule, *Opt Lett*, 27(2002)995–997.
39. Dennis M R, Polarization singularities in paraxial vector fields: morphology and statistics, *Opt Commun*, 213(2002)201–221.
40. Freund I, Polarization flowers, *Opt Commun*, 199(2001)47–63.
41. Lu T H, Chen Y F, Huang K F, Generalized hyperboloid structures of polarization singularities in Laguerre-Gaussian vector fields, *Phys Rev A*, 76(2007)063809; doi.org/10.1103/PhysRevA.76.063809.
42. Vyas S, Kozawa Y, Sato S, Polarization singularities in superposition of vector beams, *Opt Express*, 21(2013)8972; doi.org/10.1364/OE.21.008972.
43. Kumar P, Nishchal N K, Modified Mach–Zehnder interferometer for determining the high-order topological charge of Laguerre–Gaussian vortex beams, *J Opt Soc Am A*, 36(2019)1447–1455.
44. Kumar P, Nishchal N K, Self-referenced spiral interferogram using modified lateral shearing Mach–Zehnder interferometer, *Appl Opt*, 58(2019)6827–6833.
45. Rosales-Guzmán C, Ndagano B, Forbes A, A review of complex vector light fields and their applications, *J Opt*, 20(2018)123001; doi.org/10.1088/2040-8986/aaeb7d.
46. Zhan Q, Cylindrical vector beams: from mathematical concepts to applications, *Adv Opt Photon*, 1(2009)1–57.
47. Beckley A M, Brown T G, Alonso M A, Full Poincaré beams, *Opt Express*, 18(2010)10777–10785.
48. Ruchi, Senthilkumaran P, Pal S K, Phase singularities to polarization singularities, *Int J Opt*, 2020(2020)1–33.
49. Wang X, Nie Z, Liang Y, Wang J, Li T, Jia B, Recent advances on optical vortex generation, *Nanophoton*, 7(2018)1533–1556.
50. Forbes A, Dudley A, McLaren M, Creation and detection of optical modes with spatial light modulators, *Adv Opt Photon*, 8(2016)200–227.
51. Kumar P, Fatima A, Nishchal N K, Arbitrary vector beam encoding using single modulation for information security applications, *IEEE Photon Technol Lett*, 33(2021)243–246.
52. Nishchal N K, Optical Cryptosystems, (IOP Publ), 2019.

53. Zhang Y, Li P, Ma C, Liu S, Cheng H, Han L, Zhao J, Efficient generation of vector beams by calibrating the phase response of a spatial light modulator, *Appl Opt*, 56(2017)4956–4960.

54. Kumar P, Nishchal N K, Formation of singular light fields using phase calibrated spatial light modulator, *Opt Lasers Eng*, 146(2021)106720; doi.org/10.1016/j.optlaseng.2021.106720.

55. Gupta A K, Kumar P, Nishchal N K, Alfalou A, Polarization-encoded fully-phase encryption using transport of intensity equation, MDPI Electronics, 10(2021)00969; doi.org/10.3390/electronics10080969.

56. Fatima A, Nishchal N K, Image authentication using vector beam with sparse phase information, *J Opt Soc Am A*, 35(2018)1053–1062.

[*Received*: 10.06.2021; *accepted*: 01.07.2021]